

## PROPERTIES OF POTASSIUM CURRENTS AND THEIR ROLE IN MEMBRANE EXCITABILITY IN *DROSOPHILA* LARVAL MUSCLE FIBERS

BY SATPAL SINGH\* AND CHUN-FANG WU

Department of Biology, University of Iowa, Iowa City, IA 52242, USA

Accepted 20 April 1990

### Summary

The larval muscle fibers of *Drosophila* show four outward  $K^+$  currents in addition to the inward  $Ca^{2+}$  current in voltage-clamp recordings. The *Shaker* (*Sh*) and the *slowpoke* (*slo*) mutations, respectively, eliminate the voltage-activated fast  $K^+$  current ( $I_A$ ) and the  $Ca^{2+}$ -activated fast  $K^+$  current ( $I_{CF}$ ). Quinidine specifically blocks the voltage-activated delayed  $K^+$  current ( $I_K$ ) at micromolar concentrations. We used *Sh*, *slo* and quinidine to remove specifically one or more  $K^+$  currents, so as to study physiological properties of these currents not previously characterized, and to examine their role in membrane excitability. A linear relationship was observed between the peak  $I_{CF}$  and the peak  $I_{Ca}$  at different membrane potentials.  $I_{CF}$  inactivated considerably during a 140 ms pulse to +20 mV. Recovery from inactivation was not complete for up to 2 s at the holding potential of -50 mV, which is much slower than the recovery of  $Ca^{2+}$  current from inactivation. In addition to  $I_A$  and  $I_{CF}$ , two delayed  $K^+$  currents are also observed in these fibers, the voltage-activated  $I_K$  and the  $Ca^{2+}$ -activated  $I_{CS}$ . Near the end of a 500 ms depolarizing pulse, both  $I_A$  and  $I_{CF}$  are inactivated.  $Ca^{2+}$ -free and  $20\text{ mmol l}^{-1}$   $Ca^{2+}$  saline were used to examine the tail currents of the remaining  $I_K$  and  $I_{CS}$ . The tail currents of  $I_{CS}$  were slower than those of  $I_K$  and reversed between -30 and -50 mV in different fibers. We further studied the dose-dependence of the blockade of  $I_K$  by quinidine, which did not indicate a simple one-to-one binding mechanism. Current-clamp recordings from normal, *Sh*, *slo* and the double-mutant *Sh;slo* fibers suggested that  $I_{CF}$  plays a stronger role than  $I_A$  in repolarization of the larval muscle membrane. Elimination of  $I_{CF}$  facilitates the occurrence of action potentials. Further elimination of  $I_K$  prolonged the action potentials to several hundred milliseconds.

### Introduction

The existence of mutations which affect specific ionic currents in *Drosophila* provides an opportunity to analyze the properties of individual currents and to

\*Present address and address for reprint requests: Department of Biochemical Pharmacology, State University of New York at Buffalo, Buffalo, NY 14260, USA.

Key words: *Drosophila* mutants,  $K^+$  currents, quinidine, *Shaker*, *slowpoke*.

study the roles of these currents in membrane excitability. The advantage of mutational analysis can be complemented with the use of pharmacological agents that specifically block certain currents. The larval body-wall muscles in *Drosophila* support four  $K^+$  currents which can be distinguished and separated from each other with the use of mutations and drugs. These currents include two voltage-activated  $K^+$  currents, the fast  $I_A$  and the delayed  $I_K$ , and two  $Ca^{2+}$ -activated  $K^+$  currents, the fast  $I_{CF}$  and the delayed  $I_{CS}$  (Salkoff, 1983; Wu *et al.* 1983; Wu and Haugland, 1985; Gho and Mallart, 1986; Wei and Salkoff, 1986; Singh and Wu, 1989). Among these currents,  $I_A$  and  $I_{CF}$  are eliminated by the *Shaker* (*Sh*) (Salkoff and Wyman, 1981; Wu *et al.* 1983; Wu and Haugland, 1985) and the *slowpoke* (*slo*) (Elkins *et al.* 1986; Singh and Wu, 1989) mutations, respectively, and  $I_K$  is blocked by quinidine at micromolar concentrations (Singh and Wu, 1989). We have used *Sh*, *slo* and quinidine to study properties of the  $K^+$  currents that have not been described previously, and to look at their role in membrane excitability in larval body-wall muscle fibers.

Different names have been used previously for the  $Ca^{2+}$ -activated  $K^+$  currents in *Drosophila*. The fast current has been designated as  $I_{Acd}$  (Salkoff, 1983),  $I_{Ac}$  (Gho and Mallart, 1986; Wei and Salkoff, 1986) and  $I_C$  (Elkins *et al.* 1986), and the slow current as  $I_{Kc}$  (Wei and Salkoff, 1986) and  $I_C$  (Gho and Mallart, 1986). To avoid confusion and to preserve consistency with the conventional names used in other species we use the present nomenclature, i.e.  $I_{CF}$  for the fast C current and  $I_{CS}$  for the slow C current (Singh and Wu, 1989). Part of the results presented here have appeared in abstract form previously (Singh *et al.* 1986; Singh and Wu, 1987).

### Materials and methods

The wild-type strain Canton-S was used as the normal control. An extreme allele of the *Shaker* (Kaplan and Trout, 1969) locus,  $Sh^{KS133}$  (Wu and Haugland, 1985), was used for eliminating  $I_A$ . Only one allele of *slo* (Elkins *et al.* 1986) is available and was used in these experiments. These two mutant alleles have been extensively characterized in larval muscle (Wu *et al.* 1983, 1989; Wu and Haugland, 1985; Singh and Wu, 1989; Haugland and Wu, 1990).

The body-wall muscle preparation of mature third-instar larvae (Jan and Jan, 1976) was used for recordings, as described previously (Wu and Haugland, 1985; Singh and Wu, 1989). Two-microelectrode voltage-clamp recordings were made with a holding potential of  $-50$  or  $-80$  mV, as specified in the figure legends. Both the voltage-clamp and the current-clamp recordings were made at  $4^\circ\text{C}$ . Recording saline contained (in  $\text{mmol l}^{-1}$ ) 128 NaCl; 35.5 sucrose; 2 KCl and 5 Hepes, and was buffered at pH 7.1. In addition, the  $Ca^{2+}$ -free saline had  $0.5 \text{ mmol l}^{-1}$  EGTA and  $\text{MgCl}_2$  and was adjusted to  $20 \text{ mmol l}^{-1}$  for improving membrane stability (Wu and Haugland, 1985). Unless otherwise specified, the saline with  $Ca^{2+}$  contained  $20 \text{ mmol l}^{-1}$   $\text{CaCl}_2$ ,  $4 \text{ mmol l}^{-1}$   $\text{MgCl}_2$  and no EGTA. Quinidine and 4-aminopyridine (4-AP) were obtained from Sigma Chemical Co. (St Louis, MO).

The muscle fibers used in these experiments are supercontracting muscles (Osborne, 1967). The contractions induced during recordings, especially during strong depolarizations, damage the fiber quickly. Although it is possible to make reliable recordings from a fiber, it is difficult to take a single fiber through repeated experiments using different experimental paradigms or recording solutions. Therefore, all individual experiments described here were performed on separate fibers.

Voltage or current pulses were generated at intervals of 10 s by a Master-8-cp pulse generator (A.M.P.I., Jerusalem, Israel). The voltage-clamp circuit was equipped with a high-voltage head stage (model HVHD, Almost Perfect Electronics, Basel, Switzerland). The current electrode was shielded up to a few millimeters from the tip with a coaxial double shield. The inner shield was driven at the potential of the electrode and the outer shield was grounded. The voltage electrode was filled with KCl and the current electrode with a mixture of KCl and potassium citrate. The electrodes were pulled to a resistance between 5 and 15 M $\Omega$ . The current signal was recorded through the virtual ground using the amplifier M701 (WPI, New Haven, CT). The current and the voltage signals were pulse-coded using a Neurocorder unit DR-384 (Neuro Data Instruments Corp., New York, NY), and recorded using a video cassette recorder. The data were digitized and subsequently analyzed on an Apple-Macintosh II computer. Current densities in voltage-clamp recordings were obtained by normalizing the current with respect to the fiber capacitance (Haugland, 1987; Haugland and Wu, 1990). Leakage current was subtracted digitally and the initial 3 ms of recordings which contain capacitive transients have been omitted in the figures for the sake of clarity, as described previously (Singh and Wu, 1989).

## Results

### *Early membrane currents*

Voltage-clamp recordings made in 1.8 mmol l<sup>-1</sup> Ca<sup>2+</sup>, the concentration generally used in *Drosophila* saline, showed considerable variation in the Ca<sup>2+</sup>-dependent currents. This problem was overcome by increasing the external Ca<sup>2+</sup> concentration. Saline with 20 mmol l<sup>-1</sup> Ca<sup>2+</sup> was therefore used (Singh and Wu, 1989) for voltage-clamp measurements of Ca<sup>2+</sup>-dependent currents in this paper.

Early membrane currents recorded from different genotypes are shown in Fig. 1. The fast current peak seen in the normal fibers (Fig. 1A) consists of two outward currents, the voltage-activated ( $I_A$ ) and the Ca<sup>2+</sup>-activated ( $I_{CF}$ ) K<sup>+</sup> currents, and an inward Ca<sup>2+</sup>-current,  $I_{Ca}$ . As shown previously (Gho and Mallart, 1986; Singh and Wu, 1989), the outward currents mask the inward current which is therefore not apparent in the figure. Lack of  $I_{CF}$  in the *slo* mutation (Elkins *et al.* 1986; Singh and Wu, 1989) revealed the sum of  $I_A$  and  $I_{Ca}$ , in which the outward peak was reduced but the inward current was still masked (Fig. 1B). In a similar way, the *Sh* mutant that lacks  $I_A$  (Salkoff and Wyman, 1981; Wu *et al.* 1983; Wu and Haugland, 1985) showed the sum of  $I_{CF}$  and  $I_{Ca}$  (Fig. 1C). The

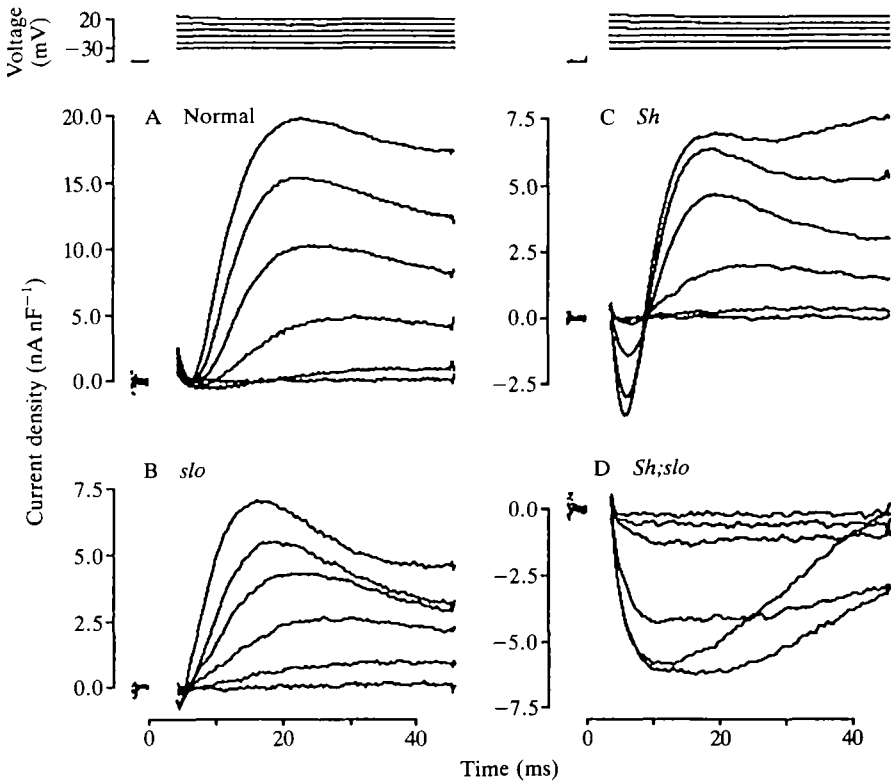


Fig. 1. Voltage-clamp recordings of the early currents from the larval muscle fibers in *Drosophila*. Superimposed traces show currents elicited by voltage steps to  $-30$ ,  $-20$ ,  $-10$ ,  $0$ ,  $10$  and  $20$  mV from a holding potential of  $-50$  mV in saline containing  $20 \text{ mmol l}^{-1} \text{ Ca}^{2+}$ . The early current in the normal fibers (A) consists of  $I_A$ ,  $I_{CF}$  and  $I_{Ca}$ . Among these, the inward  $I_{Ca}$  is not apparent as it has been masked by the two outward currents  $I_A$  and  $I_{CF}$ . The *Sh* mutation eliminates  $I_A$  and shows the sum of  $I_{CF}$  and  $I_{Ca}$  (C). Similarly, the sum of  $I_A$  and  $I_{Ca}$  is seen in *slo* which lacks  $I_{CF}$  (B). The *Sh;slo* double mutant lacks both  $I_A$  and  $I_{CF}$  and thus unmasks the inward  $\text{Ca}^{2+}$  current  $I_{Ca}$  (D), which is otherwise obscured by the two outward currents. The current is shown as normalized to the membrane capacitance. Approximately the first 3 ms of recordings show capacitive transients and have been omitted from the figure for the sake of clarity. Note the difference in the current scale for the normal fibers and the rest of the fibers. For this and the following figures, all experiments were conducted at  $4^\circ\text{C}$ .

inward  $\text{Ca}^{2+}$  current can be seen during the short interval before it is masked by the outward  $I_{CF}$ . Since these fibers have both  $I_A$  and  $I_{CF}$ , the total outward current is stronger than in *Sh* or in *slo*. Elimination of both the outward currents ( $I_A$  and  $I_{CF}$ ) in the *Sh;slo* double mutant (Fig. 1D) unmasks the inward  $I_{Ca}$ .

#### *I<sub>CF</sub> inactivation*

Both  $I_A$  and  $I_{CF}$  in larvae (Wu and Haugland, 1985; Gho and Mallart, 1986) and

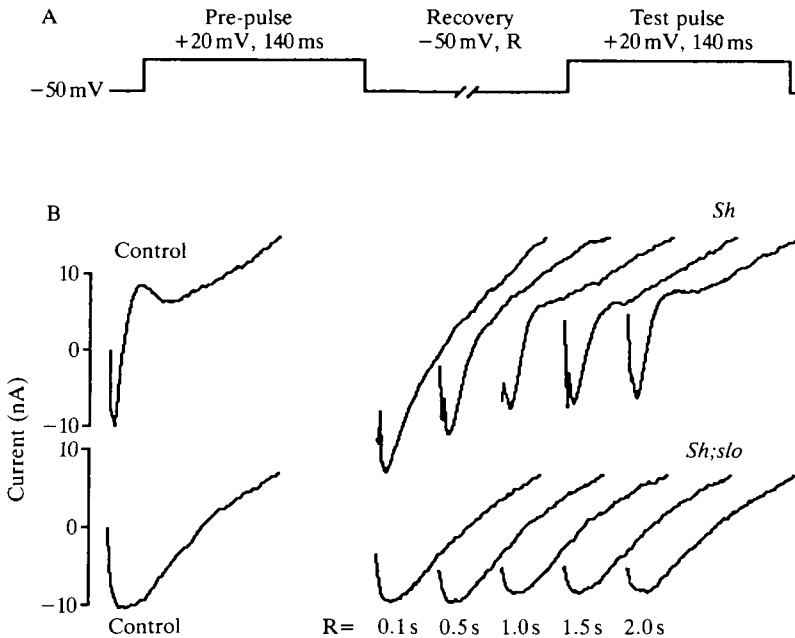


Fig. 2. Inactivation and recovery of  $I_{CF}$ . (A) Pulse paradigm. R indicates recovery time between the pre-pulse and the test pulse, each of 140 ms duration, to +20 mV from the holding and the recovery potential of -50 mV. (B) Sequential recordings were obtained from the same fibers. Recovery times of 0.1, 0.5, 1.0, 1.5 and 2.0 s were given, as shown beneath the different traces. Recordings from *Sh;slo* show  $I_{Ca}$  and those from *Sh* show the contribution of both  $I_{Ca}$  and  $I_{CF}$ . The shortest recovery time given in the experiment, 100 ms, was enough for the recovery of  $I_{Ca}$  from whatever, if any, inactivation took place. In contrast, recovery of  $I_{CF}$  was not complete even after 2 s at the holding potential. In this figure, the current is shown in nA and not as current density and the time scale is indicated by the pulse paradigm.

in adults (Salkoff, 1983; Salkoff and Wyman, 1983) have been shown to inactivate with membrane depolarization. The  $I_{CF}$  inactivation in larvae is almost complete at a membrane potential of -20 mV (Gho and Mallart, 1986), a potential at which  $I_{Ca}$  or  $I_{CF}$  have still not been activated. This implies that the  $I_{CF}$  inactivation is voltage-dependent and not  $Ca^{2+}$ -dependent. However, there is no study on the recovery of  $I_{CF}$  from inactivation in larvae. This was studied by using different experimental protocols and recovery times in recordings from *Sh* (44 fibers) and *Sh;slo* (36 fibers). Fig. 2 shows the effect of a 140 ms pre-pulse to +20 mV on  $I_{CF}$  and  $I_{Ca}$ . Their recovery, after different times at the holding potential of -50 mV, was tested by an identical test pulse. The pulse paradigm is shown in Fig. 2A. The first traces in both the *Sh* and the *Sh;slo* recordings in Fig. 2B show the membrane current during the pre-pulse, which serves as a control. Since  $I_K$  and  $I_{CS}$  rise slowly with a delay, the early phase (0–40 ms) of this current mainly consists of the inward  $I_{Ca}$  in *Sh;slo* and the sum of  $I_{Ca}$  and  $I_{CF}$  in *Sh*. The traces on the right show

membrane currents in response to the test pulse, after the indicated recovery period at  $-50$  mV.  $I_{CF}$  was considerably inactivated by the pre-pulse. Note that the first test pulse (after 0.1 s recovery time) shows stronger inward current than the control current seen with the pre-pulse in *Sh* (Fig. 2B). Since the *Sh* fibers lack  $I_A$ , the inactivation of  $I_{CF}$  unmask the inward current to a greater degree. Even if inactivation did occur in  $I_{Ca}$  during the pre-pulse, it recovered during the first 100 ms, as indicated by recordings in *Sh; slo*. In contrast,  $I_{CF}$  showed clear inactivation which did not recover completely within 2 s (compare *Sh* and *Sh; slo* in Fig. 2B). The recovery from inactivation of  $I_{CF}$  was slower than that of  $I_A$ , which shows substantial recovery within 1 s at a comparable temperature (Wu and Haugland, 1985). The main result is that the recovery of  $I_{CF}$  from inactivation may not be linked to that of  $I_{Ca}$ .

#### Relationship between peak $I_{CF}$ and $I_{Ca}$

The possibility of extracting  $I_{CF}$  with the use of mutations enabled us to look at the relationship between this current and the inward  $Ca^{2+}$  current that is responsible for its activation. The current-voltage relationship for the extracted  $I_{CF}$  is given in Fig. 3A. The values for  $I_{CF}$  were obtained by subtracting the averaged current densities recorded in *Sh; slo* from those recorded in *Sh*. The

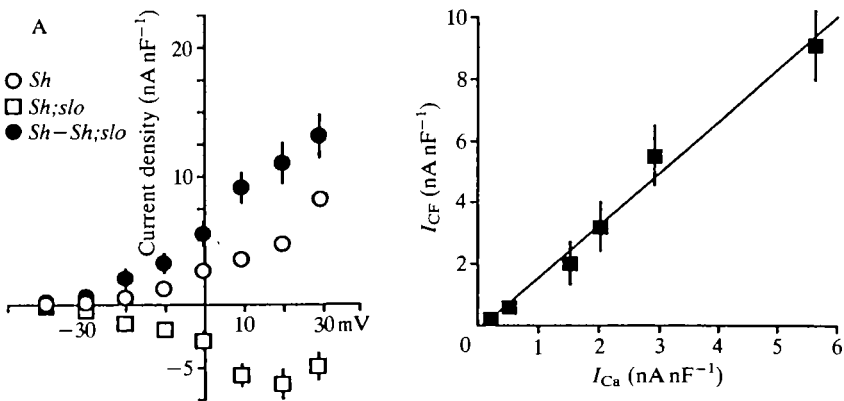


Fig. 3. (A) Current-voltage relationship for  $I_{CF}$ . Currents were normalized to fiber capacitance. Peak values for the fast current plotted here were calculated as described in the text. Current from *Sh; slo* fibers ( $\square$ ) lacks both  $I_A$  and  $I_{CF}$ . Current from *Sh* fibers ( $\circ$ ) lacks  $I_A$  but not  $I_{CF}$ . Digital subtraction of the *Sh; slo* current from the *Sh* current thus gives  $I_{CF}$  ( $\bullet$ ). Recordings represent averages from a number of fibers ( $F$ ) taken from a number of larvae ( $L$ ). *Sh; slo*:  $F=7$ ,  $L=3$ ; *Sh*:  $F=10$ ,  $L=4$ . Bars represent standard error of the mean. (B) Relationship between the  $Ca^{2+}$ -activated fast  $K^+$  current  $I_{CF}$  and the inward current  $I_{Ca}$ . Same data as shown in A. Mean  $\pm$  S.E.M. for  $I_{CF}$  is plotted against mean  $I_{Ca}$  at the membrane potentials of  $-40$ ,  $-30$ ,  $-20$ ,  $-10$ ,  $0$  and  $+10$  mV. Measurements of  $I_{Ca}$  become less reliable at more positive potentials because the inward peak becomes masked by the more rapid rise of the delayed outward currents. The continuous line represents linear regression.

current for *Sh* is shown as the early peak of the outward current at different membrane potentials. For the purpose of subtraction, the inward  $I_{Ca}$  in *Sh;slo* was measured at the time when a peak occurred for the outward current in *Sh* at the corresponding voltage. This time was a few milliseconds after the actual inward peak in *Sh;slo* (see Fig. 1C and D), which gives values very similar to the ones shown in Fig. 3A.

Fig. 3B shows the relationship between  $I_{CF}$  and  $I_{Ca}$ , determined as described for Fig. 3A. It shows a linear dependence of  $I_{CF}$  on  $I_{Ca}$ . This is consistent with a one-to-one correspondence between the  $Ca^{2+}$  entering the fiber and the opening of individual  $I_{CF}$  channels. A linear relationship between the amount of  $Ca^{2+}$  injected directly into the cell and the value of the  $Ca^{2+}$ -activated  $K^+$  current has also been reported in the dorsal unpaired median neurons in the cockroach (Thomas, 1984). However, the data cannot be taken as conclusive evidence for a one-to-one correspondence, because the amount of free  $Ca^{2+}$  in the cytosol depends on the influx of  $Ca^{2+}$ , on the nature of the  $Ca^{2+}$  sequestering process and on a number of other factors.

#### *The $Ca^{2+}$ -activated slow $I_{CS}$*

In addition to the fast  $Ca^{2+}$ -activated  $I_{CF}$ , the larval muscle fibers in *Drosophila* also show a slow  $Ca^{2+}$ -activated outward  $I_{CS}$  (Gho and Mallart, 1986; Singh and Wu, 1989). We performed experiments with  $0\text{ mmol l}^{-1} Ca^{2+}$  (20 fibers for *Sh* and 10 fibers for *Sh;slo*) or  $20\text{ mmol l}^{-1} Ca^{2+}$  (19 fibers for *Sh* and 13 fibers for *Sh;slo*) in the saline.  $I_{CS}$  was observed in recordings made in saline with  $20\text{ mmol l}^{-1} Ca^{2+}$ . *Sh* and *Sh;slo* gave similar results because  $I_{CF}$  is almost completely inactivated during the 500 ms pulse used in these experiments (Fig. 2 shows inactivation produced by a 140 ms pulse) and the contamination from residual  $I_{CF}$  is expected to be minor. Fig. 4A shows the voltage-activated  $I_K$  in  $Ca^{2+}$ -free saline, which reaches a steady state before the end of the 500 ms pulse. In Fig. 4B,C, the delayed outward current recorded in saline with  $Ca^{2+}$  consisted of  $I_K$  and  $I_{CS}$ .  $I_{CS}$  can be seen as changes in the overall amplitude of the slow outward current and the tail currents after the voltage pulse has ended. Unlike  $I_{CF}$ ,  $I_{CS}$  did not inactivate, and in fact continued to rise for at least 500 ms. This contrast between the fast and the slow  $Ca^{2+}$ -activated outward currents,  $I_{CF}$  and  $I_{CS}$ , parallels the difference between the two voltage-activated outward currents, the fast transient  $I_A$  and the delayed sustained  $I_K$ .

The tail currents were recorded by stepping the membrane potential to +20 mV and then repolarizing it to different voltages (Fig. 4). The tail currents immediately after the end of the voltage pulse are either inward or outward, depending on the membrane potential reached. Inward tail currents are expected if the membrane potential is repolarized below the reversal potential for the current, and outward tails are expected if it is above the reversal potential. Only outward tail currents were seen in recordings made in  $Ca^{2+}$ -free saline (Fig. 4A). This is because  $I_K$  does not show inward tail currents as there is strong rectification (Wu and Haugland, 1985). Inward tails were seen when recordings were made in the

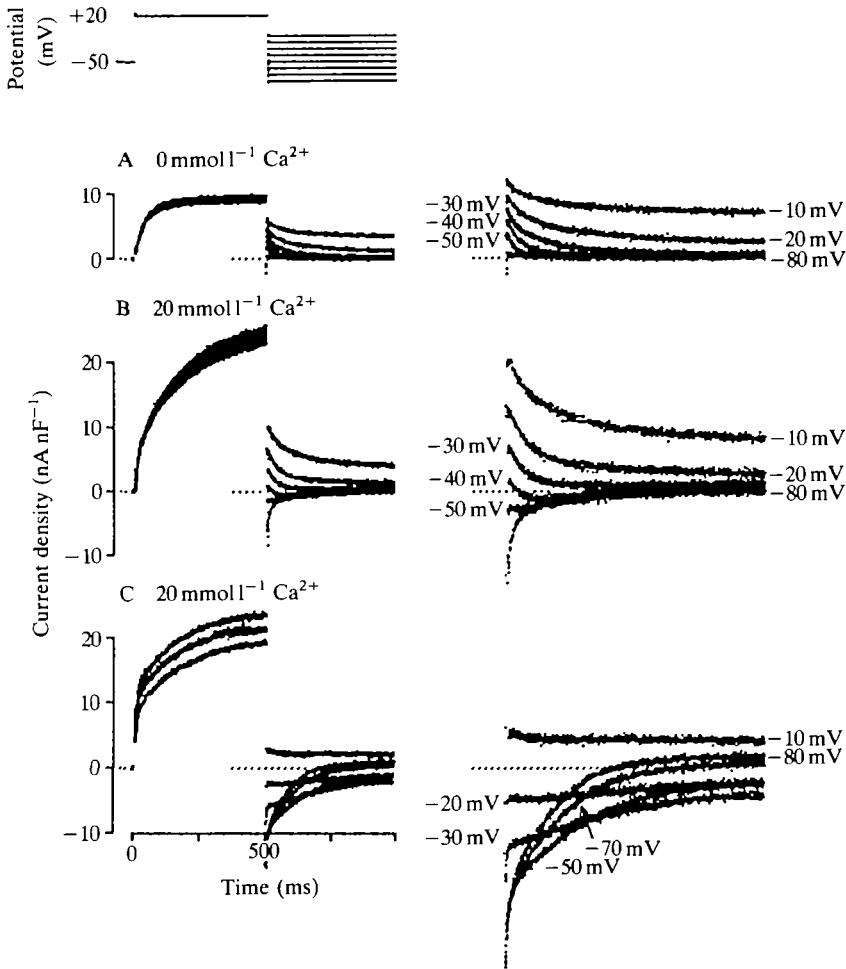


Fig. 4

presence of Ca<sup>2+</sup>. Fig. 4B shows inward tail currents for I<sub>CS</sub> and combined outward tail currents for I<sub>K</sub> and I<sub>CS</sub>. Inward tails are seen for potentials up to -40 mV. At -30 mV, the tails were completely outward. At this potential, I<sub>CS</sub> makes only a marginal contribution to the outward tail in Fig. 4B, as can be seen by comparing with the tail at -30 mV in Fig. 4A. The reversal potential for I<sub>CS</sub> in Fig. 4B thus lies between -40 and -30 mV, near to -30 mV. In different fibers, the reversal potential ranged between -30 and -50 mV.

In some fibers, depolarization by repeated test pulses showed a cumulative effect on the outward current and gave rise to more complex tail currents. Fig. 4C shows an example where inward tail current is seen up to -20 mV. The outward tail for -10 mV (Fig. 4C) is also not as strong as the I<sub>K</sub> tail at the same voltage (Fig. 4A). The reversal potential for the current in addition to I<sub>K</sub> in this case seems to be more positive than -10 mV. A possible interpretation of this is suggested in the Discussion.



Fig. 4. Measurement of tail currents from *Sh* fibers in  $\text{Ca}^{2+}$ -free saline and in saline containing  $20 \text{ mmol l}^{-1} \text{Ca}^{2+}$ . The voltage signal is shown at the top to indicate the pulse paradigm. The left part of the figure shows the membrane currents during the voltage step as well as the tail currents. The right side of the figure shows the tail currents magnified twofold on the time scale as well as the current scale. Membrane potential was stepped from the holding value of  $-50 \text{ mV}$  to  $+20 \text{ mV}$  for  $500 \text{ ms}$ . The membrane was then repolarized to different levels as specified along the magnified tail currents. Tail currents at selected voltages are shown for the sake of clarity. The horizontal dotted lines represent the zero level of the current when no active current is going across the membrane. (A) Recordings in  $\text{Ca}^{2+}$ -free saline show only the voltage-activated current  $I_K$ , as  $I_A$  is missing because these are *Sh* fibres. Only outward tail currents are seen, as  $I_K$  channels show strong rectification. (B,C) Recordings with  $20 \text{ mmol l}^{-1} \text{Ca}^{2+}$  in the saline. Activation of  $I_{CS}$  is indicated by the continuing rise of outward currents during the pulse and the changes in the tail currents, which now include an additional component due to  $I_{CS}$ , as indicated by the appearance of the inward tails. This additional component in most fibers showed a reversal potential between  $-30$  and  $-40 \text{ mV}$  (B). In some fibers, the outward current showed cumulative effects during repeated pulses (only the first three traces are shown in C to avoid cluttering) and the tail currents showed a stronger negative component which reversed at more positive potentials. In the case shown here, the additional tail component reversed near  $-10 \text{ mV}$  (C).

---

#### *The relative role of $I_A$ and $I_{CF}$ in membrane excitability*

The ability to eliminate individual  $\text{K}^+$  currents by means of mutations and pharmacological agents allows an analysis of the role of different currents in membrane excitability. Mutational elimination of  $I_A$  and  $I_{CF}$  has been used in adult dorsal longitudinal flight muscles (DLM) of *Drosophila* for this purpose (Elkins and Ganetzky, 1988). We used the lack of  $I_A$  in *Sh* and the lack of  $I_{CF}$  in *slo* to study the role of these currents in the excitability of larval muscle fibers. This was done by looking at the membrane potential in response to constant current injection.

Regenerative potentials have recently been demonstrated in larval preparations in which air was supplied through tracheoles to maintain the resting potentials up to  $-80 \text{ mV}$  (Yamaoka and Ikeda, 1988). Most previous reports, which used un-aerated preparations, described lower resting potentials and only graded potentials in response to current injection in normal physiological saline, which contains  $1.8 \text{ mmol l}^{-1} \text{Ca}^{2+}$  (Suzuki and Kano, 1977; Wu and Ganetzky, 1988). We found that regenerative responses were easier to elicit when the resting potential was sufficiently negative, either in a freshly dissected preparation or because of injection of a hyperpolarizing current even in the absence of aeration. Recordings were made from the normal (4 fibers), *Sh* (9 fibers) and *slo* (13 fibers). Fig. 5 shows recordings made in fibers with the resting potential kept near  $-60$  to  $-70 \text{ mV}$  by injecting hyperpolarizing current. The regenerative peak in these recordings is more pronounced in *slo* and in *Sh*. A smaller amount of current was required to elicit regenerative potentials in *slo* as compared to *Sh*. This indicates that  $I_{CF}$  is more effective than  $I_A$  in repolarizing the regenerative potential supported by  $I_{Ca}$ .

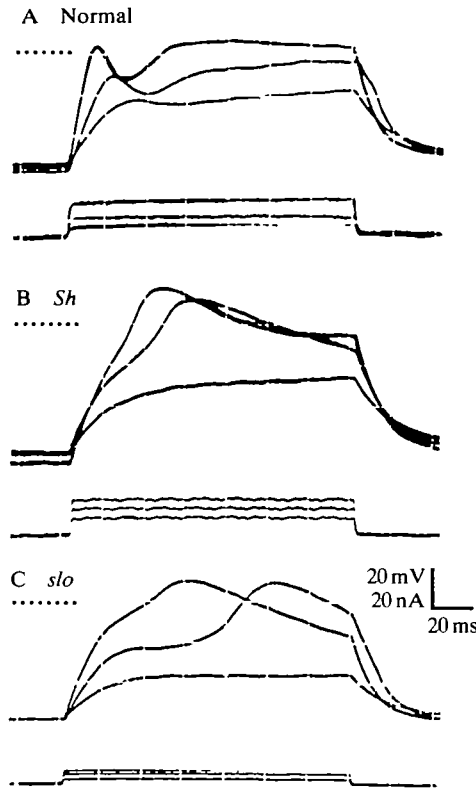


Fig. 5. Membrane potential (upper traces) in response to constant current injection (lower traces). The saline contained  $1.8 \text{ mmol l}^{-1} \text{ Ca}^{2+}$ . The resting membrane potential in these recordings was maintained around  $-60$  to  $-70$  mV by a hyperpolarizing current. The zero potential level is represented by the horizontal dotted lines. The *Sh* (B) and the *slo* (C) fibers show more clear regenerative potentials than the normal ones (A). The amount of current needed for eliciting regenerative potentials is less for *slo* than for *Sh*. The fiber sizes used in these three experiments are different. For example, the size of the particular *Sh* fiber shown in B is larger than that of the particular normal fiber shown in A. Therefore, a comparable amount of current charges the membrane faster in the normal fiber than in the *Sh* fiber shown here.

The relative role of different outward currents can be seen more clearly by using saline containing  $20 \text{ mmol l}^{-1} \text{ Ca}^{2+}$ . With increased  $\text{Ca}^{2+}$  concentration, pronounced regenerative potentials could be elicited when one or more outward currents were removed by mutations or drugs. This could be achieved without aeration in preparations with resting potentials as low as  $-20$  mV. Fig. 6 shows recordings made in saline containing  $20 \text{ mmol l}^{-1} \text{ Ca}^{2+}$  without injection of hyperpolarizing current. The normal fibers showed graded potentials in response to increasing amounts of current injection (Fig. 6A) and did not show action potentials. Elimination of  $I_A$  by *Sh* led to increased depolarization, which was still graded in nature (Fig. 6B). However, when  $I_{CF}$  was eliminated by the *slo* mutation, the fibers underwent all-or-none action potentials (Fig. 6C). This is

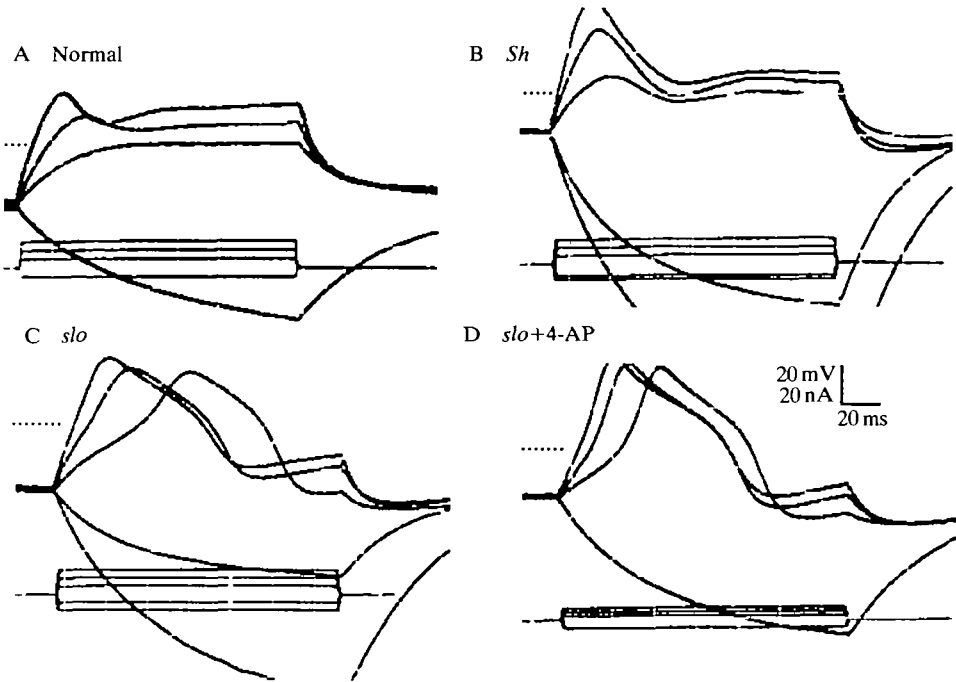


Fig. 6. Membrane potentials in response to current injection with  $20 \text{ mmol l}^{-1} \text{ Ca}^{2+}$  in the saline. No hyperpolarizing holding current was applied. The horizontal dotted line represents the zero potential level. The normal (A) and the *Sh* (B) fibers show graded responses to current injection, the latter showing a stronger initial depolarization. Elimination of  $I_{CF}$  in *slo* fibers gives rise to action potentials (C). If 4-aminopyridine (4-AP,  $100 \mu\text{mol l}^{-1}$ ), which blocks  $I_A$ , is added to the saline, *slo* fibers require less current injection to give rise to action potentials (D).

consistent with the observation shown in Fig. 5 that  $I_{CF}$  plays a stronger role than  $I_A$  in repolarizing the membrane. As expected, *slo* fibers treated with 4-AP ( $100 \mu\text{mol l}^{-1}$ ), which preferentially blocks  $I_A$  at this concentration, also exhibit all-or-none action potentials, but requiring even less injection of current (Fig. 6D) than *slo* (Fig. 6C). The number of fibers tested was 11 for the normal, 10 for *Sh*, 16 for *slo* and 22 for *slo* with 4-AP.

#### Blockade of $I_K$ by quinidine

Quinidine, which blocks different  $\text{K}^+$  currents in several systems (Fishman and Spector, 1981; Hermann and Gorman, 1984; Imaizumi and Giles, 1987), blocks  $I_K$  in *Drosophila* (Singh and Wu, 1989). The inset in Fig. 7 shows membrane currents in response to voltage steps from the holding potential of  $-80 \text{ mV}$  to  $-10$ ,  $+10$  and  $+30 \text{ mV}$  in  $\text{Ca}^{2+}$ -free saline with and without quinidine.  $I_A$  was removed by the use of *Sh*, and  $0.1 \text{ mmol l}^{-1}$  quinidine substantially blocked the only remaining current  $I_K$ . This concentration of quinidine has earlier been shown not to block  $I_A$ ,

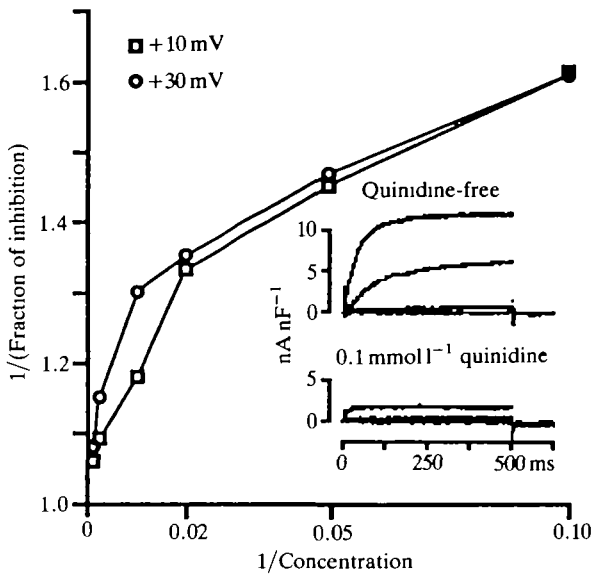


Fig. 7. Blockade of  $I_K$  by quinidine represented in a double-reciprocal plot between the fraction of inhibition and the quinidine concentration (in  $\mu\text{mol l}^{-1}$ ). The inset shows the reduction of  $I_K$  due to  $0.1 \text{ mmol l}^{-1}$  quinidine, as recorded from *Sh* fibers in  $\text{Ca}^{2+}$ -free saline. Membrane currents are shown in response to voltage steps to  $-10$ ,  $+10$  and  $+30 \text{ mV}$  from the holding potential of  $-80 \text{ mV}$ . This part of the figure is adopted from Singh and Wu (1989). The values of  $I_K$  in the plot were determined from the amplitude at the end of a  $500 \text{ ms}$  pulse to  $+10$  or  $+30 \text{ mV}$ , as specified in the figure. The mean values of  $I_K$  were derived from a number of fibers (at different concentrations in  $\mu\text{mol l}^{-1}$ ): 7 (0); 3 (10); 6 (20); 2 (50); 12 (100); 3 (500) and 3 (1000).

$I_{CF}$  or  $I_{CS}$  (Singh and Wu, 1989). The double-reciprocal plot in Fig. 7 shows the effect of different concentrations of quinidine on the amplitude of  $I_K$ . Quinidine at  $10 \mu\text{mol l}^{-1}$  reduced  $I_K$  by more than half. In this plot, the reciprocal of the fraction of inhibition is plotted against the reciprocal of quinidine concentration in micromoles per liter. A linear relationship would signify a simple saturation with one-to-one binding of quinidine molecules to the  $I_K$  channels. Fig. 7 shows a deviation from a linear relationship. Although  $I_K$  is blocked more than 50% by  $10 \mu\text{mol l}^{-1}$  quinidine (as indicated by the upper-most point in the plot), even  $1.0 \text{ mmol l}^{-1}$  quinidine leaves some current intact (the lower-most point in the plot). It is not clear at this stage if this is a manifestation of sub-populations of  $I_K$  with different sensitivity to quinidine.

Some  $\text{K}^+$  channel blockers are known to show voltage-dependent action. The extent of inhibition by quinidine was examined at  $+10$  and  $+30 \text{ mV}$  in *Drosophila*. The plot shows small differences at the two potentials (Fig. 7). These differences could not be substantiated statistically, owing to the small sample sizes, but were far less pronounced than the voltage-dependence reported for 4-AP (Yeh *et al.* 1976) and tetraethylammonium (Armstrong, 1971).

*The role of  $I_K$  in membrane excitability*

Selective blockade of  $I_K$  by quinidine provided an opportunity to examine the role of this current in determining the membrane potential. Fig. 8 shows current-clamp recordings in saline containing  $20 \text{ mmol l}^{-1} \text{ Ca}^{2+}$  and  $100 \text{ } \mu\text{mol l}^{-1}$  quinidine. In the absence of quinidine, normal and *Sh* fibers did not show action potentials, as discussed above. Removal of  $I_K$  by quinidine did not show a strong effect except for a slight regenerative potential, as indicated by a shoulder in *Sh* after the end of the current injection (Fig. 8B). In the case of *slo* and *Sh;slo*, regenerative potentials were initiated even during weak current pulses. After the end of the pulse, the regenerative potential was sustained for hundreds of milliseconds (Fig. 8C,D). The duration of the prolonged depolarization was highly

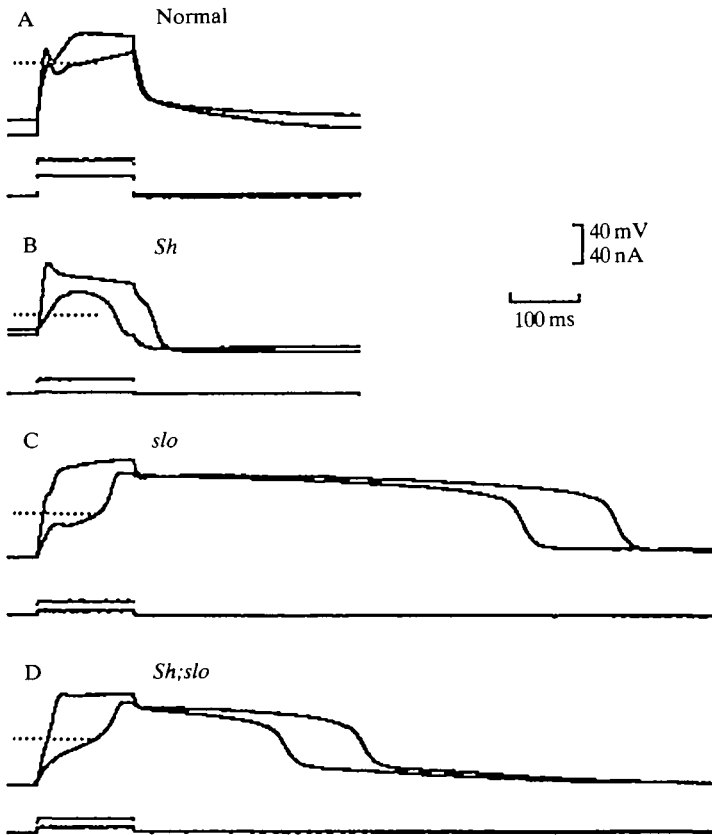


Fig. 8. Effect of quinidine on the membrane potential. The saline contained  $20 \text{ mmol l}^{-1} \text{ Ca}^{2+}$ . Responses to 140 ms current pulses in the presence of  $100 \text{ } \mu\text{mol l}^{-1}$  quinidine are shown. The dotted horizontal lines indicate the zero potential level. The normal (A) and the *Sh* (B) fibers repolarized soon after the current pulse was over. In contrast, the regenerative potentials initiated during the current pulse in *slo* (C) and *Sh;slo* (D) fibers were sustained for several hundred milliseconds after the end of the current pulse.

variable even between fibers of the same genotype and no consistent differences were found between *slo* and *Sh;slo*. Elimination of  $I_K$  thus prevents repolarization of  $Ca^{2+}$  regenerative potentials initiated either by the lack of  $I_{CF}$  alone or by the elimination of both  $I_{CF}$  and  $I_A$  (compare Fig. 8 with Fig. 6). The number of fibers tested was 9 for the normal, 8 for *Sh*, 10 for *slo* and 7 for *Sh;slo*.

## Discussion

### *Properties of $K^+$ currents*

The availability of the two mutations, *Sh* and *slo*, allows a comparison between  $I_A$  and  $I_{CF}$  underlying the early phase of the membrane current. Fig. 1B,C shows that the generation of the  $Ca^{2+}$ -activated  $I_{CF}$  is preceded by the voltage-activated  $I_A$ . Presumably,  $I_{CF}$  requires  $Ca^{2+}$  influx following  $I_{Ca}$  activation, whereas  $I_A$  is activated by membrane depolarization without a lag following  $I_{Ca}$  activation. As previously reported (Gho and Mallart, 1986),  $I_{CF}$ , like  $I_A$ , was inactivated by membrane depolarization.  $I_{CF}$  recovery from inactivation followed a time course much slower than that of  $I_{Ca}$  recovery (Fig. 2), suggesting a process independent of the availability of cytosolic free  $Ca^{2+}$ .

The late outward currents consist of  $I_K$  and  $I_{CS}$ .  $I_K$  can be isolated by using *Sh* in  $Ca^{2+}$ -free saline. This allows an analysis of the effect of quinidine on  $I_K$ . A double-reciprocal plot between the fractional inhibition and the quinidine concentration did not indicate a linear relationship (Fig. 7). This observation suggests that there are different sub-populations of  $I_K$  channels with different sensitivities to quinidine, a possibility that requires further investigation.

As mentioned above,  $I_K$  does not show inward tail currents because of rectification (Fig. 4A). Outward currents are seen at potentials more positive than  $-60$  mV but not at a potential of  $-70$  mV. The reversal potential for this current is therefore between  $-60$  and  $-70$  mV, consistent with the earlier reported reversal potential for  $I_K$  (Wu and Haugland, 1985). Fig. 4B shows both outward and inward tail currents, recorded in saline containing  $Ca^{2+}$ . In different fibers, the component contributed by  $I_{CS}$  reversed at a potential between  $-50$  and  $-30$  mV (see Results). This is consistent with  $I_{CS}$  being a  $K^+$  current in larvae (Gho and Mallart, 1986) as well as in adults (Wei and Salkoff, 1986). The currents observed in the presence of  $Ca^{2+}$  show a greater degree of variation in some fibers. Fig. 4C shows such a fiber with a reversal potential that is more positive than  $-10$  mV. Such a reversal potential was generally associated with stronger tail currents as well as a cumulative effect on the variable outward currents during repeated voltage pulses (Fig. 4C). This type of behavior was generally elicited in fibers that were relatively leaky, which may be an indication of deterioration or damage. A more positive reversal potential may be accounted for by the presence of yet another set of channels or a non-selective conductance in addition to the  $I_{CS}$  channels.

### *The roles of $K^+$ currents in membrane excitability*

Yamaoka and Ikeda (1988) have recently shown that the tracheole aeration of

the larval preparation is essential in maintaining the resting potential of the muscle fibers and in initiating a regenerative response. Lack of aeration results in a drop in the resting potential from about  $-80$  mV to about  $-30$  mV within 1 h at room temperature. It is known that the resting potentials in many insect muscles are maintained below the  $K^+$  equilibrium potential by electrogenic pumps (Huddart and Wood, 1966; Rheuben, 1972; Henon and Ikeda, 1981). The metabolic state, which would depend upon effective aeration, is thus expected to influence the resting potential. However, it is not clear if the effect of aeration on the regenerative response is due to the membrane potential, which would determine the state of channel inactivation, or to a direct deteriorative effect on channel machinery or to some other cellular factors. Recordings in this study and in other reports (Jan and Jan, 1976; Suzuki and Kano, 1977; Wu and Ganetzky, 1988) have been made in the larval preparation without tracheole aeration. Our recordings from muscle fibers with resting potentials at different levels indicated that the metabolic condition was probably not a prerequisite for regenerative responses. Regenerative responses were easier to elicit in fibers with resting potentials between  $-60$  and  $-70$  mV, maintained by injection of hyperpolarizing currents or by low temperature ( $4^\circ\text{C}$ ) in freshly dissected preparations. For example, regenerative potentials could be seen in *Sh* fibers only if the resting potential was more negative than  $-60$  mV (compare Figs 5B and 6B; note the inflexion points in Fig. 5B). An effect of resting potential on the regenerative events is expected since the  $Ca^{2+}$  channels mediating inward current inactivate to different degrees depending upon the extent of membrane depolarization. The main aim of the present study was to compare the relative role of different  $K^+$  currents in membrane excitability. We found clear differences between the consequences of eliminating different currents on excitability, even without tracheole aeration. However, it is important to investigate these differences under normal physiological conditions with effective aeration.

An important consideration is the free  $Ca^{2+}$  concentration around the fibers as well as inside the fibers. This can be a source of variation in the  $Ca^{2+}$ -activated  $K^+$  currents as it can affect the amount of  $Ca^{2+}$  influx and the  $Ca^{2+}$  available to trigger these currents. From electron microscopic observations (Jan and Jan, 1976; C.-F. Wu, unpublished data), the larval muscle fibers are enveloped by relatively little connective tissue. In addition, ion replacement and drug additions to the recording saline show immediate effects, indicating a lack of effective diffusion barriers (Wu and Haugland, 1985; Haugland, 1987; Singh and Wu, 1989; Wu *et al.* 1989). The level of intracellular free  $Ca^{2+}$  can conceivably vary in relation to metabolic state, e.g. a weakened sequestering mechanism, and affect the  $Ca^{2+}$  concentration gradient across the plasma membrane as well as the available free  $Ca^{2+}$  for activating  $I_{CF}$  and  $I_{CS}$ . It will be important to determine the free  $Ca^{2+}$  level directly, employing other available techniques in future investigations.

Interactions between the outward and the inward currents determine the membrane potential in response to a current stimulus. The inward current depolarizes the membrane and the outward current counteracts this by repolariz-

ing the membrane. As in other arthropod species, the inward current in *Drosophila* muscles is carried by  $\text{Ca}^{2+}$  (Suzuki and Kano, 1977; Salkoff and Wyman, 1983; Elkins *et al.* 1986; Gho and Mallart, 1986). A tetrodotoxin-sensitive inward current was recently suggested by current-clamp experiments (Yamaoka and Ikeda, 1988). It remains to be determined by voltage-clamp experiments whether it is a  $\text{Na}^+$  inward current. The outward currents in *Drosophila* muscles consist of two voltage-activated ( $I_A$  and  $I_K$ ) and two  $\text{Ca}^{2+}$ -activated ( $I_{CF}$  and  $I_{CS}$ )  $\text{K}^+$  currents. The effectiveness of different  $\text{K}^+$  currents in repolarizing the membrane depends on their channel density (current amplitude) and their kinetic characteristics. Because of these differences, they give rise to a variety of excitability patterns.

An ability to manipulate different currents, by the use of mutations and drugs, provides an opportunity to examine the role of individual currents in excitability. The two fast outward currents ( $I_A$  and  $I_{CF}$ ) in the normal fibers limit the membrane depolarization immediately after the initiation of the current injection. As compared to the normal muscles, therefore, a lack of  $I_A$  in the *Sh* muscles allowed a larger initial depolarization with the same amount of current injection (compare Fig. 6A and 6B). However, removal of  $I_{CF}$  alone, in *slo*, had a greater effect, resulting in action potentials, even at a low resting membrane potential (see Fig. 6C). This implies that  $I_{CF}$  plays a more effective role in membrane repolarization than does  $I_A$  during prolonged current injections. It is known that  $I_A$  inactivates rapidly (Salkoff and Wyman, 1983; Wu and Haugland, 1985) and is effective in delaying membrane excitation (Salkoff and Wyman, 1983; Elkins and Ganetzky, 1988) but would not have a prolonged repolarizing effect. Although  $I_{CF}$  is similar in magnitude to  $I_A$ , its activation is coupled to the activation of  $I_{Ca}$ . In addition, it inactivates at more depolarized potentials (Gho and Mallart, 1986) and with a slower time course (S. Singh and C.-F. Wu, unpublished observations) than  $I_A$ . The effect of  $I_A$  removal became more apparent only when the resting potential was more negative (Fig. 5B) or when  $I_{CF}$  was also removed (action potentials in Fig. 6D require less current injection compared to Fig. 6C). These observations on the relative role of  $I_A$  and  $I_{CF}$  in the excitability of larval muscles are consistent with the earlier conclusions on their role in the adult flight muscles (Elkins and Ganetzky, 1988).

In contrast to the early currents, the slow outward currents activate with delay but show little inactivation. The role of  $I_K$  in muscle repolarization is revealed by the use of quinidine. In normal and *Sh* fibers, blockade of  $I_K$  by quinidine led to only marginal differences. However, when the membrane undergoes an action potential, as when  $I_{CF}$  is removed in *slo* or *Sh;slo*,  $I_K$  assumes an important role in repolarization. The action potentials lasted only a few tens of milliseconds when  $I_K$  was present (Fig. 6C,D) but lasted for several hundred milliseconds when  $I_K$  was blocked by quinidine (Fig. 8C,D). In the experiments shown in Figs 6 and 8,  $I_A$  and  $I_{CF}$  are expected to have inactivated to a great extent by the end of the current pulse. The repolarization of the action potential, once initiated, thus depends mainly on  $I_K$  and  $I_{CS}$ . With the further removal of  $I_K$ , the termination of the



prolonged action potential after the end of the current pulse will depend primarily on the amplitudes of  $I_{Ca}$  and  $I_{CS}$ , and how they change with time. The membrane during this prolonged depolarization is presumably in an unstable equilibrium and the time taken by the membrane to repolarize varied considerably, regardless of the genotype (data not shown). The sustained action potential is similar to, but less prolonged than that seen in the larval muscle fibers treated with tetraethylammonium (Suzuki and Kano, 1977; S. Singh and C.-F. Wu, unpublished observations), which blocks all four  $K^+$  currents in this system to different degrees (Wu and Haugland, 1985; Gho and Mallart, 1986). So far no mutations or drugs remove  $I_{CS}$  specifically. Such a possibility would be very useful for determining the role of  $I_{CS}$  in membrane excitability.

This work was supported by USPHS grants NS-15350, NS-18500 and NS-26528.

### References

- ARMSTRONG, C. M. (1971). Interaction of tetraethylammonium ion derivatives with the potassium channels of giant axons. *J. gen. Physiol.* **58**, 413–437.
- ELKINS, T. AND GANETZKY, B. (1988). The roles of potassium currents in *Drosophila* flight muscles. *J. Neurosci.* **8**, 428–434.
- ELKINS, T., GANETZKY, B. AND WU, C.-F. (1986). A *Drosophila* mutation that eliminates a calcium-dependent potassium current. *Proc. natn. Acad. Sci. U.S.A.* **83**, 8415–8419.
- FISHMAN, M. C. AND SPECTOR, I. (1981). Potassium current suppression by quinidine reveals additional calcium currents in neuroblastoma cells. *Proc. natn. Acad. Sci. U.S.A.* **78**, 5245–5249.
- GHO, M. AND MALLART, A. (1986). Two distinct calcium-activated potassium currents in larval muscle fibers of *Drosophila melanogaster*. *Pflügers Arch. ges. Physiol.* **407**, 526–533.
- HAUGLAND, F. N. (1987). A voltage clamp analysis of membrane potassium currents in larval muscle fibers of the *Shaker* mutants of *Drosophila*. PhD thesis, University of Iowa.
- HAUGLAND, F. N. AND WU, C. F. (1990). A voltage-clamp analysis of gene-dosage effects of the *Shaker* locus on larval muscle potassium currents in *Drosophila*. *J. Neurosci.* (in press).
- HENON, B. K. AND IKEDA, K. (1981). Changes in membrane properties of the *Drosophila* dorsal longitudinal flight muscles induced by sodium pump inhibitors. *J. exp. Biol.* **90**, 175–183.
- HERMANN, A. AND GORMAN, A. L. F. (1984). Action of quinidine on ionic currents of molluscan pacemaker neurons. *J. gen. Physiol.* **83**, 919–940.
- HUDDART, H. AND WOOD, D. W. (1966). The effect of DNP on the resting potential and ionic content of some insect skeletal muscle fibers. *Comp. Biochem. Physiol.* **18**, 681–688.
- IMAIZUMI, Y. AND GILES, W. R. (1987). Quinidine-induced inhibition of transient outward current in cardiac muscle. *Am. J. Physiol.* **253**, H704–H708.
- JAN, L. Y. AND JAN, Y. N. (1976). Properties of the larval neuromuscular junction in *Drosophila melanogaster*. *J. Physiol., Lond.* **262**, 189–214.
- KAPLAN, W. D. AND TROUT III, W. E. (1969). The behavior of four neurological mutants of *Drosophila*. *Genetics* **61**, 399–409.
- OSBORNE, M. P. (1967). Supercontraction in the blowfly larva: an ultrastructural study. *J. Insect Physiol.* **13**, 1471–1482.
- RHEUBEN, M. (1972). The resting potential of moth muscle fiber. *J. Physiol. Lond.* **225**, 529–554.
- SALKOFF, L. (1983). *Drosophila* mutants reveal two components of fast outward current. *Nature* **302**, 249–251.
- SALKOFF, L. AND WYMAN, R. (1981). Genetic modification of potassium channels in *Drosophila Shaker* mutants. *Nature* **293**, 228–230.
- SALKOFF, L. AND WYMAN, R. (1983). Ionic currents in *Drosophila*. *J. Physiol., Lond.* **337**, 687–709.

- SINGH, S. AND WU, C.-F. (1987). Genetic and pharmacological separation of four potassium currents in *Drosophila* larvae. *Soc. Neurosci. Abstr.* **13**, 579.
- SINGH, S. AND WU, C.-F. (1989). Complete separation of four potassium currents in *Drosophila*. *Neuron* **2**, 1325–1329.
- SINGH, S., WU, C.-F. AND GANETZKY, B. (1986). Interactions among different  $K^+$  and  $Ca^{2+}$  currents in normal and mutant *Drosophila* larval muscles. *Soc. Neurosci. Abstr.* **12**, 559.
- SUZUKI, N. AND KANO, M. (1977). Development of action potential in larval muscle fibers in *Drosophila melanogaster*. *J. cell. Physiol.* **93**, 383–388.
- THOMAS, M. V. (1984). Voltage-clamp analysis of a calcium-mediated potassium conductance in cockroach (*Periplaneta americana*) central neurons. *J. Physiol., Lond.* **350**, 159–178.
- WEI, A. AND SALKOFF, L. (1986). Occult *Drosophila* calcium channels and twinning of calcium and voltage-activated potassium channels. *Science* **233**, 780–782.
- WU, C.-F. AND GANETZKY, B. (1988). Genetic and pharmacological analyses of potassium channels in *Drosophila*. In *Neurotox '88: Molecular Basis of Drug and Pesticide Action* (ed. G. G. Lunt), pp. 311–323. Amsterdam: Elsevier.
- WU, C.-F., GANETZKY, B., HAUGLAND, F. N. AND LIU, A.-X. (1983). Potassium currents in *Drosophila*: Different components affected by mutations of two genes. *Science* **220**, 1076–1078.
- WU, C.-F. AND HAUGLAND, F. N. (1985). Voltage clamp analysis of membrane currents in larval muscle fibers of *Drosophila*. Alteration of potassium currents in *Shaker* mutants. *J. Neurosci.* **5**, 2626–2640.
- WU, C.-F., TSAI, M.-C., CHEN, M.-L., ZHONG, Y., SINGH, S. AND LEE, C. Y. (1989). Actions of dendrotoxin on  $K^+$  channels and its synergistic effect on neuromuscular transmission with  $K^+$  channel-specific drugs and mutations in *Drosophila melanogaster*. *J. exp. Biol.* **147**, 21–41.
- YAMAOKA, K. AND IKEDA, K. (1988). Electrogenic responses elicited by transmembrane depolarizing current in aerated body wall muscles of *Drosophila melanogaster* larvae. *J. comp. Physiol.* **163**, 705–714.
- YEH, J. Z., OXFORD, G. S., WU, C. H. AND NARAHASHI, T. (1976). Interactions of aminopyridines with potassium channels of squid axon membranes. *Biophys. J.* **16**, 77–81.